Synthesis and Electrochemistry of Tetraphenylporphyrins Containing an Antimony−Carbon σ-Bond

Karl M. Kadish,*,† Marie Autret,† Zhongping Ou,† Kin-ya Akiba,*,‡ Shuji Masumoto,‡ Ryosuke Wada,‡ and Yohsuke Yamamoto‡

Department of Chemistry, University of Houston, Houston, Texas 77204-5641, and Department of Chemistry, Faculty of Science, Hiroshima University, 1-3-1 Kagamiyama, Higashi-Hiroshima 739, Japan

Received December 1, 1995[⊗]

The following five antimony(V) tetraphenylporphyrins with σ-bonded antimony−carbon bonds were synthesized: $[(TPP)Sb(CH_3)_2]^+PF_6^-$, $[(TPP)Sb(OCH_3)(OH)]^+PF_6^-$, $[(TPP)Sb(CH_3)(OH)]^+ClO_4^-$, $[(TPP)Sb(CH_3)(OCH_3)]^+ClO_4^-$, and $[(TPP)Sb(CH_3)(F)]^+PF_6^-$. Each compound is stable toward air and moisture and has a high melting point (>250 °C). The electrochemistry and spectroelectrochemistry of these σ-bonded porphyrins were examined in benzonitrile or dichloromethane containing 0.1 M tetrabutylammonium perchlorate as supporting electrolyte and the data compared to those for three previously synthesized OEP derivatives containing similar σ-bonded and/or anionic axial ligands. Each porphyrin shows two reversible reductions and up to a maximun of one oxidation within the potential window of the solvent. Spectroelectrochemical data indicate formation of a porphyrin π anion radical upon the first reduction as do ESR spectra of the singly reduced species. However, a small amount of the Sb(III) porphyrin products may be generated via a chemical reaction following electron tranfer. An X-ray crystallographic analysis of $[(TPP)Sb(CH_3)(F)]^+PF_6^-$ is also presented: monoclinic, space group $C2/c$, $Z = 8$, $a = 24.068(5)$ Å, $b = 19.456(4)$ Å, $c = 18.745(3)$ Å, $\beta = 94.69(2)°$, $R = 0.056$.

Introduction

Porphyrins with metal-carbon bonds have been studied in detail,[1] but until a recent report[2] on the synthesis of $[(OEP)Sb(R)(L)]^+Y^-$ ($R = CH_3, C_2H_5$; $L = CH_3, OH^-$), nothing was known about σ-bonded porphyrins with group 15 central metal ions. Our work on these types of porphyrins and hypervalent organic molecules[3] has now been extended to include antimony−alkyl σ-bonded tetraphenylporphyrins of the type $[(TPP)Sb(R)(L)]^+Y^-$ where $R = CH_3$ or OCH_3^-, $L = CH_3$, OH^-, OCH_3^-, or F^-, and $Y = PF_6$ or ClO_4. The bonding around the antimony atom in these porphyrins is hypervalent, and the complexes can be represented as (12-Sb−6) systems.[4] Each porphyrin was examined by electrochemistry, ESR spectroscopy and UV−visible spectroelectrochemistry. Redox potentials are also reported for related $[(OEP)Sb(R)(L)]^+Y^-$ complexes which were previously synthesized.[2]

Experimental Section

Instrumentation. Cyclic voltammetry was carried out with an EG&G Model 173 potentiostat or an IBM Model EC 225 voltammetric analyzer. Current−voltage curves were recorded on an EG&G Princeton Applied Research Model RE-0151 X-Y recorder. A three-electrode system was used and consisted of a glassy carbon or platinum button working electrode, a platinum wire counter electrode, and a saturated calomel reference electrode (SCE). This reference electrode was separated from the bulk of the solution by a fritted-glass bridge filled with the solvent/supporting electrolyte mixture. All potentials are referenced to the SCE. UV−visible spectroelectrochemical experiments were performed with a home-built platinum thin-layer electrode of the type described in the literature.[5] Potentials were applied and monitored with an EG&G Princeton Applied Research Model 173 potentiostat. Time-resolved UV−visible spectra were recorded with a Princeton Instrument RY-1024 diode array detector and an ST 120 detector controller. Melting points were measured with a Yanagimoto micromelting point apparatus and were uncorrected. ^{1}H NMR (400 MHz) and ^{19}F NMR (376MHZ) spectra were recorded on a JEOL EX-400 spectrometer. ^{1}H NMR (90MHz) and ^{19}F NMR (85 MHz) spectra were recorded on a Hitachi R-90H spectrometer. Chemical shifts are reported (δ scale) with respect to internal tetramethylsilane for ^{1}H spectra and with respect to internal fluorotrichloromethane for ^{19}F spectra. UV−visible spectra were recorded on a Shimadzu UV-2200 spectrophotometer. High-resolution mass spectra were recorded on a JEOL SX-102A spectrometer. Elemental analyses were performed on a Perkin-Elmer 2400 CHN elemental analyzer. Column chromatography was carried out on Merck alumina neutral 1077.

Chemicals. Benzonitrile (PhCN) was purchased from Aldrich Chemical Co. and distilled over P_2O_5 under vacuum prior to use.

† University of Houston.
‡ Hiroshima University.
[⊗] Abstract published in *Advance ACS Abstracts,* May 1, 1996.

(1) Recent reviews: Guilard, R.; Kadish, K. M. *Chem. Rev.* **1988**, *88*, 1121. Guilard, R.; Lecomte, C.; Kadish, K. M. *Struct. Bonding (Berlin)* **1987**, *64*, 205. References to recent reports on main group element porphyrins having element−carbon bond(s) follow. Al: Inoue, S.; Takeda, N. *Bull. Chem. Soc. Jpn.* **1977**, *50*, 984. Ga: Kadish, K. M.; Boisselier-Cocolios, B.; Cocolios, P.; Guilard, R. *Inorg. Chem.* **1985**, *24*, 2139. Kadish, K. M.; Boisselier-Cocolios, B.; Coutsolelos, A.; Mitaine, P.; Guilard, R. *Inorg. Chem.* **1985**, *24*, 4521. In: Cocolios, P.; Guilard, R.; Bayeul, D.; Lecomte, C. *Inorg. Chem.* **1985**, *24*, 2058. Tabard, A.; Guilard, R.; Kadish, K. M. *Inorg. Chem.* **1986**, *25*, 4277. Tl: Henrick, K.; Matthews, R. W.; Tasker, P. A. *Inorg. Chem.* **1977**, *16*, 3293. Kadish, K. M.; Tabard, A.; Zrineh, A.; Ferhat, M.; Guilard, R. *Inorg. Chem.* **1987**, *26*, 2459. Ge: Kadish, K. M.; Xu, Q. Y.; Barbe, J.-M.; Anderson, J. E.; Wang, E.; Guilard, R. *J. Am. Chem. Soc.* **1987**, *109*, 7705. Cloutour, C.; Lafargue, D.; Pommier, J. C. *J. Organomet. Chem.* **1978**, *161*, 327. Si: Kadish, K. M.; Xu, Q. Y.; Barbe, J.-M.; Guilard, R. *Inorg. Chem.* **1988**, *27*, 1191. Sn: Cloutour, C.; Lafargue, D.; Pommier, J. C. *J. Organomet. Chem.* **1980**, *190*, 35.

(2) Akiba, K.-y.; Onzuka, Y.; Itagaki, M.; Hirota, H.; Yamamoto, Y. *Organometallics* **1994**, *13*, 2800.

(3) (a) Yamamoto, Y.; Nadano, R.; Itagaki, M.; Akiba, K.-y. *J. Am. Chem. Soc.* **1995**, *117*, 8287. (b) Yamamoto, Y.; Chen, X.; Kojima, S.; Ohdoi, K.; Kitano, M.; Doi, Y.; Akiba, K.-y. *J. Am. Chem. Soc.* **1995**, *117*, 3922. (c) Yamamoto, Y.; Chen, X.; Akiba, K.-y. *J. Am. Chem. Soc.* **1992**, *114*, 7906. (d) Yamamoto, Y.; Fujikawa, H.; Fujishima, H.; Akiba, K.-y. *J. Am. Chem. Soc.* **1989**, *111*, 2276. (e) Akiba, K.-y.; Fujikawa, H.; Sunaguchi, Y.; Yamamoto, Y. *J. Am. Chem. Soc.* **1987**, *109*, 1245; (f) Akiba, K.-y.; Okinaka, T.; Nakatani, M.; Yamamoto, Y. *Tetrahedron Lett.* **1987**, *28*, 3367.

(4) Perkins, C. W.; Martin, J. C.; Arduengo, A. J.; Lau, W.; Algeria, A.; Kochi, J. K. *J. Am. Chem. Soc.* **1980**, *102*, 7753.

(5) Lin, X. Q.; Kadish, K. M. *Anal. Chem.* **1985**, *57*, 1498.

S0020-1669(95)01538-2 CCC: $12.00

Absolute dichloromethane (CH_2Cl_2) was obtained over molecular sieves from Fluka Chemical Co. and used without further purification. Tetra-*n*-butylammonium perchlorate (TBAP) was purchased from Sigma Chemical Co., recrystallized from ethanol, and dried under vacuum at 40 °C for at least 1 week prior to use.

(TPP)SbBr. $(TPP)H_2$ (6.06 g, 9.76 mmol) and $SbBr_3$ (14.00 g, 39.0 mmol) were heated under reflux for 1 day under Ar in a solution containing 120 mL of dry dichloromethane and 10 mL of 2,6-dimethylpyridine. Water (20 mL), hexane (30 mL), and then dichloromethane (30 mL) were added to the solution, and the mixture was filtered through Celite. The aqueous layer was extracted with dichloromethane (3 × 50 mL), and the organic layer was dried over $MgSO_4$. After filtration, the organic solvent was evaporated to give 7.58 g (TPP)SbBr (yield 95%): mp 221−235 °C dec; ^{1}H NMR ($CDCl_3$) δ (ppm) 7.77−7.85 (m, 12 H), 8.26−8.35 (m, 8 H), 9.26 (s, 8 H).

$[(TPP)Sb(CH_3)_2]^+PF_6^-$. Trimethylaluminum, $(CH_3)_3Al$ (a 15% solution in hexane, 0.25 mL, 0.355 mmol), was added to 15 mL of (TPP)SbBr (26.6 mg, 0.033 mmol) in CH_2Cl_2 under nitrogen at room temperature. The mixture was stirred for 7 days at room temperature, after which it was treated with cold water and then filtered through Celite. The organic layer was removed and the aqueous layer extracted with dichloromethane (3 × 50 mL). The combined organic layer was dried over $MgSO_4$. After filtration, the solvent was evaporated. The residue was dissolved in CH_3OH, and potassium hexafluorophosphate (5 equiv) in CH_3OH was added to the solution. Crude $[(TPP)Sb(CH_3)_2]^+PF_6^-$ was recrystallized from dichloromethane/ether (1:3) to give purple crystals (10 mg, 40%) of $[(TPP)Sb(CH_3)_2]^+PF_6^-$: mp 281−288 °C dec; UV−visible (CH_2Cl_2) λ ($\epsilon \times 10^{-3}$) 350 (25.7), 416 (42.4), 438 (498), 581 (13.5), 624 (25.9); ^{1}H NMR ($CDCl_3$) δ (ppm) −6.00 (s, 6 H), 7.88−7.96 (m, 12 H), 8.28−8.36 (m, 8 H), 9.36 (s, 8 H). Anal. Calcd for $C_{46}H_{34}N_4SbPF_6 \cdot CH_2Cl_2$: C, 56.77; H, 3.65; N, 5.63. Found: C, 56.69; H, 3.85; N, 5.81.

$[(TPP)Sb(OCH_3)(OH)]^+PF_6^-$. To a solution of (TPP)SbBr (1.86 g, 2.28 mmol) in 300 mL of CH_3OH was added 1.0 mL (17.5 mmol) of aqueous hydrogen peroxide (35%) at room temperature. The mixture was stirred for 6 h at room temperature and the solvent then evaporated. After addition of CH_2Cl_2 (50 mL) and water (50 mL), the organic layer was removed and the aqueous layer extracted with CH_2Cl_2 (3 × 50 mL). The combined organic layer was dried over $MgSO_4$. After filtration, the solvent was evaporated to give crude $[(TPP)Sb(OCH_3)(OH)]^+OH^-$ (1.75 g, 97%). An exchange of the OH^- counteranion by PF_6^- on $[(TPP)Sb(OCH_3)(OH)]^+OH^-$, using potassium hexafluorophosphate, quantitatively gave $[(TPP)Sb(OCH_3)(OH)]^+PF_6^-$ (CH_2C1_2/*n*-hexane; 1:1): mp >300 °C; ^{1}H NMR ($CDCl_3$) δ (ppm) −2.27 (s, 3 H), 7.78−7.93 (m, 12 H), 8.22−8.59 (m, 8 H), 9.39 (s, 8 H). Anal. Calcd for $C_{45}H_{32}N_4O_2SbPF_6$: C, 58.27; H, 3.48; N, 6.04. Found: C, 57.90; H, 3.37; N, 5.98.

$[(TPP)Sb(CH_3)(OH)]^+ClO_4^-$. Trimethylaluminum (15% solution in hexane, 6.5 mL, 9.18 mmol) was added to a solution of $[(TPP)Sb(OCH_3)(OH)]^+OH^-$ (1.76 g, 2.20 mmol) in 30 mL of CH_2Cl_2 under Ar at room temperature. The mixture was stirred for 3 days, treated with cold water, and then filtered through Celite. The organic layer was removed and the aqueous layer extracted with dichloromethane (3 × 50 mL). The combined organic layer was dried over $MgSO_4$. After filtration, the solvent was evaporated and the residue chromatographed (benzene/methanol; 15:1) to give $[(TPP)Sb(CH_3)(OH)]^+OH^-$ (1.12 g, 65%). Counteranion exchange of $[(TPP)Sb(CH_3)(OH)]^+OH^-$ with sodium perchlorate quantitatively gave $[(TPP)Sb(CH_3)(OH)]^+ClO_4^-$ (CH_2Cl_2/benzene; 1:4): mp 164−169 °C dec; ^{1}H NMR ($CDCl_3$) δ (ppm) −5.44 (s, 3 H), 7.85−7.92 (m, 12 H), 8.37−8.39 (m, 8 H), 9.39 (s, 8 H). Anal. Calcd for $C_{45}H_{32}N_4O_5ClSb \cdot 1.5C_6H_6$: C, 65.97; H, 4.20; N, 5.70. Found: C, 66.12; H, 4.18; N, 5.54.

$[(TPP)Sb(CH_3)(OCH_3)]^+ClO_4^-$. To a solution of $[(TPP)Sb(CH_3)(OH)]^+OH^-$ (160 mg, 0.208 mmol) in 20 mL of dry dichloromethane was added 0.25 mL (2.93 mmol) of oxalyl chloride at room temperature under Ar. The mixture was stirred for 2 h at room temperature and the solvent evaporated. Crude $[(TPP)Sb(CH^3)(Cl)]^+Cl^-$ could be used for further reactions. $[(TPP)Sb(CH_3)(Cl)]^+Cl^-$**:** mp 275−279 °C dec; ^{1}H NMR ($CDCl_3$) δ (ppm) −4.82 (s, 3 H), 7.80−8.01 (m, 12 H), 8.17−8.53 (m, 8 H), 9.45 (s, 8 H).

Table 1. Crystallographic Data for $[(TPP)Sb(CH_3)(F)]^+PF_6^-$

formula	$C_{45}H_{31}N_4SbPF_7 \cdot 1.5CH_2Cl_2$
mol wt	1040.90
cryst syst	monoclinic
space group	*C*2/*c*
cryst dimens, mm	0.55 × 0.50 × 0.30
color	violet
habit	plate
a, Å	24.068(5)
b, Å	19.456(4)
c, Å	18.745(3)
α, deg	90
β, deg	94.69(2)
γ, deg	90
V, Å^3	8748(3)
Z	8
D_{obs}, D_{calc}, g cm^{-3}	1.6, 1.58
abs coeff, cm^{-1}	7.73
F(000)	4168
radiation; λ, Å	Mo Kα; 0.710 73
temp, °C	23 ± 1
$2\theta_{max}$, deg	55
scan rate, deg/min	6.0
data collected	$+h,+k,\pm l$
no. of total data collcd, unique, obsd	10719, 10068, 7162 ($I > 3\sigma(I)$)
R_{int}	0.03
no. of params refined	572
R, R_w, S[a]	0.056, 0.065, 2.04
max shift in final cycle	0.47
final diff map max, e/Å^3	1.49 (near solvent)

[a] Function mimimized was $\sum[w(|F_o|^2 - |F_c|^2)^2]$, where $w = 1.0/(\sigma|F_o|^2 + 0.0003|F_o|^2)$. $R = \sum(||F_o| - |F_c||)/\sum|F_o|$. $R_w = [\sum w(|F_o| - |F_c|)^2/\sum|F_o|^2]^{1/2}$.

Dry CH_3OH (10 mL) was added to crude $[(TPP)Sb(CH_3)(Cl)]^+Cl^-$ (60.4 mg, 0.0769 mmol) at room temperature under Ar. The mixture was stirred for 2 days at room temperature, the solvent evaporated, and the residue chromatographed (acetonitrile/benzene/methanol; 30:15:1) to give $[(TPP)Sb(CH_3)(OCH_3)]^+Cl^-$ (48 mg, 81%). Counteranion exchange of $[(TPP)Sb(CH_3)(OCH_3)]^+Cl^-$ with sodium perchlorate quantitatively gave $[(TPP)Sb(CH_3)(OCH_3)]^+ClO_4^-$ which was recrystallized from CH_2Cl_2/benzene (1:3): mp 160−170 °C dec; ^{1}H NMR ($CDCl_3$) δ (ppm) −5.30 (s, 3 H), −2.64 (s, 3 H), 7.77−7.99 (m, 12 H), 8.29−8.46 (m, 8 H), 9.42 (s, 8 H). Anal. Calcd for $C_{46}H_{34}N_4O_5ClSb$: C, 62.78; H, 3.89; N, 6.37. Found: C, 62.69; H, 4.07; N, 6.12.

$[(TPP)Sb(CH_3)(F)]^+PF_6^-$. To a solution of $[(TPP)Sb(CH_3)(OH)]^+PF_6^-$ (111 mg, 0.122 mmol) in 4 mL of dry dichloromethane was added 0.2 mL (1.41 mmol) of oxalyl bromide at room temperature under Ar. The mixture was stirred for 15 min at room temperature and the solvent evaporated. Crude $[(TPP)Sb(CH_3)(Br)]^+PF_6^-$ could be used for further reactions. $[(TPP)Sb(CH_3)(Br)]^+PF_6^-$: mp 259−265 °C dec; ^{1}H NMR ($CDCl_3$) δ (ppm) −4.85 (s, 3 H), 7.84−8.03 (m, 12 H), 8.14−8.61 (m, 8 H), 9.42 (s, 8 H).

Dry *t*-BuOH (0.3 mL, 3.18 mmol) and acetonitrile (3 mL) were added to crude $[(TPP)Sb(CH_3)(Br)]^+PF_6^-$ (preparation described above) at room temperature under Ar. The mixture was heated under reflux for 2.5 days and the solvent evaporated. Potassium hexafluorophosphate (141 mg, 0.766 mmol) and acetonitrile (15 mL) were added to the residue, and the mixture was stirred for 1 day at room temperature. After dichloromethane (50 mL) and water (50 mL) were added, the organic layer separated and the aqueous layer was extracted with dichloromethane (3 × 50 mL). The combined organic layer was dried over $MgSO_4$. After filtration, the solvent was evaporated and the residue recrystallized from dichloromethane/*n*-hexane (1:1) to give purple crystals (100 mg, 90%) of $[(TPP)Sb(CH_3)(F)]^+PF_6^-$: mp 283−294 °C dec; ^{1}H NMR ($CDCl_3$) δ (ppm) −4.90 (s, 3 H), 7.84−7.95 (m, 12 H), 8.24−8.50 (m, 8 H), 9.47 (s, 8 H). Anal. Calcd for $C_{45}H_{31}N_4SbPF_7 \cdot 1.5CH_2Cl_2$: C, 53.66; H, 3.29; N, 5.38 Found: C, 53.77; H, 2.99; N, 5.38.

X-ray Structure Determination of $[(TPP)Sb(CH_3)(F)]^+PF_6^-$. Crystal data and numerical details of the structure determinations are given in Table 1. A crystal suitable for X-ray structure determination was mounted on a Mac Science MXC3 diffractometer and irradiated

Scheme 1

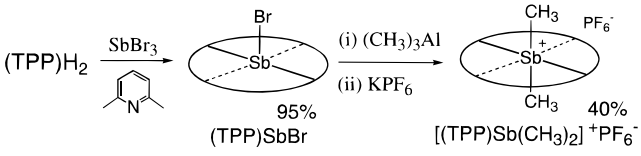

with graphite-monochromated Mo Kα radiation ($\lambda = 0.710\ 73$ Å) for data collection. Lattice parameters were determined by least-squares fitting of 26 reflections with $31° < 2\theta < 35°$. Data were collected with the $2\theta/\omega$ scan mode. All data were corrected for absorption[6] and extinction.[7] The structures were solved by direct methods with the program Monte Carlo-Multan.[8] Refinement on *F* was carried out by full-matrix least-squares. All non-hydrogen atoms were refined with anisotropic thermal parameters except those of dichloromethane (1.5 mol), which was incorporated in the crystal lattice and was disordered, so that only part of the structure could be included in the refinement on fixed positions. The hydrogen atoms were included in the refinement on calculated positions (C−H = 1.0 Å) riding on their carrier atoms with isotropic thermal parameters. All computations were carried out on a Titan-750 computer.

Results and Discussion

Synthesis. Initial attempts to introduce the antimony ion into the tetraphenylporphyrin, $(TPP)H_2$, with $SbBr_3$ under pyridine reflux[9] gave in our hands, at most, a 14% yield of (TPP)SbBr. Therefore, 2,6-lutidine was used in place of pyridine to reduce any nucleophilic attack on $SbBr_3$ and (TPP)SbBr. Dichloromethane was used as a cosolvent, and this modified method gave (TPP)SbBr in a 95% yield.

Synthesis of the Sb(V) tetraphenylporphyrins followed published methods for preparation of the OEP derivatives containing the same types of axial ligands.[2,10] For example, the reaction of (TPP)SbBr with $(CH_3)_3Al$ in CH_2Cl_2 gave $[(TPP)Sb(CH_3)_2]^+PF_6^-$ in a 40% yield after purification by column chromatography (neutral alumina) and counteranion exchange. The mechanism for formation of $[(TPP)Sb(CH_3)_2]^+PF_6^-$ should be similar to that for the corresponding octaethylporphyrins.[2] The dimethyl compound is stable to atmospheric moisture and chromatographic treatment and was characterized by HRMS, elemental analysis, and ^1H NMR, the last of which showed the expected Sb−CH_3 signal at $\delta = -6.00$ ppm, due to the ring current effect of the porphyrin nucleus.[11]

The treatment of (TPP)SbBr with aqueous hydrogen peroxide in CH_3OH gave $[(TPP)Sb(OCH_3)(OH)]^+PF_6^-$ (Scheme 1) in 97% yield after counteranion exchange.

The reaction of $[(TPP)Sb(OCH_3)(OH)]^+OH^-$ with $(CH_3)_3Al$ in CH_2Cl_2 gave $[(TPP)Sb(CH_3)(OH)]^+ClO_4^-$ in 65% yield after counteranion exchange. The monoalkylated compound is also stable to moisture and was purified by column chromatography (neutral alumina). The reaction of R_3Al with (TPP)SbBr and $[(TPP)Sb(OCH_3)(OH)]^+OH^-$ can lead to different alkylated products, as is also the case for the octaethylporphyrin analogues.[2]

Scheme 2

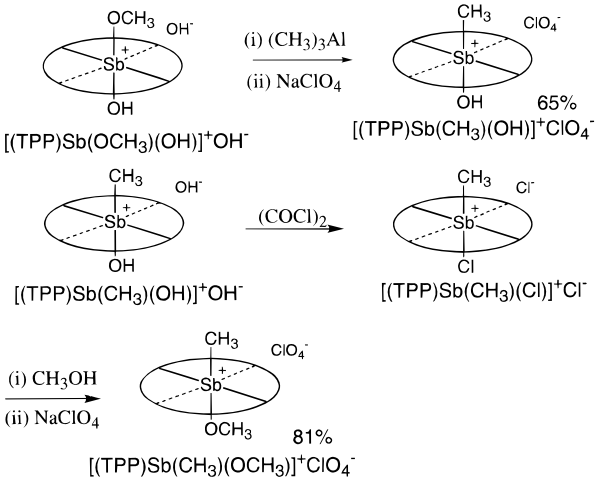

Scheme 3

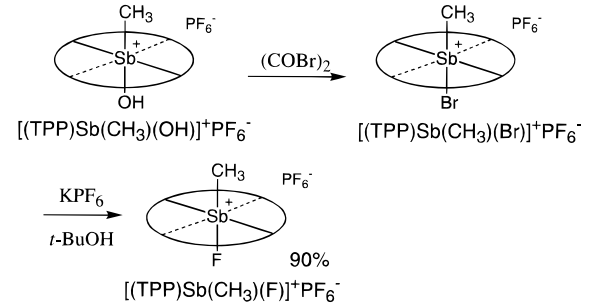

The reaction of oxalyl chloride with $[(TPP)Sb(CH_3)(OH)]^+OH^-$ (Scheme 2) gives $[(TPP)Sb(CH_3)(Cl)]^+Cl^-$, which reacts with CH_3OH to afford $[(TPP)Sb(CH_3)(OCH_3)]^+ClO_4^-$ in an 81% yield after counteranion exchange. Finally, $[(TPP)Sb(CH_3)(F)]^+PF_6^-$ is obtained when $[(TPP)Sb(CH_3)(Br)]^+PF_6^-$ is refluxed with a small amount of *t*-BuOH in acetonitrile (see Scheme 3).[12]

X-ray Crystal Structure of $[(TPP)Sb(CH_3)(F)]^+PF_6^-$. Crystals of $[(TPP)Sb(CH_3)(F)]^+PF_6^-$ suitable for X-ray analysis were obtained by recrystallization from dichloromethane/*n*-hexane (1:1). X-ray structural analysis of the compound was carried out on the basis of *C2/c*. Refinement led to the final values of $R = 0.056$ and $R_w = 0.065$. In this case, the solvent, dichloromethane (population 1.5), was found incorporated in the crystal lattice. Figure 1 shows the ORTEP drawing with the solvent omitted for clarity. Selected bond lengths and bond angles are listed in Table 2. The geometry about the antimony atom is distorted octahedral, where the length of the axial Sb−CH_3 bond (2.115(6) Å) is comparable to the Sb−CH_3 bond lengths in $[(OEP)Sb(CH_3)_2]^+PF_6^-$ (2.121(7) and 2.061(9) Å).[2] It is interesting to note that the antimony atom lies at 0.201 Å out of the plane of the four nitrogens (Δ4N)[13] toward the carbon atom. It is interesting to note that the direction of doming is

(6) Furusaki, A. *Acta Crystallogr.* **1979**, *A35*, 220.
(7) Katayama, C. *Acta Crystallogr.* **1986**, *A42*, 19.
(8) Coppens, P.; Hamilton, W. C. *Acta Crystallogr.* **1970**, *A26*, 71.
(9) (a) Inoue, H.; Sumitani, M.; Sekita, A.; Hida, M. *J. Chem. Soc., Chem. Commun.* **1987**, 1681. (b) Inoue, H. Private communication.
(10) The corresponding methylantimony(III) porphyrin could be observed as an initial product during the reaction, but this intermediate was rapidly converted to the dimethylantimony(V) species. The mechanism for conversion is still unclear, but two pathways might be suggested. The first is that the lone electron pair on the Sb ion of the intermediate reacts with a second molecule of $(CH_3)_3Al$ to form another intermediate, which then rearranges in the presence of an additional $(CH_3)_3Al$ molecule to give the final dimethylantimony(V) porphyrin product. A second possibility is that the Sb(III) intermediate is oxidized by trace oxygen during the reaction and the oxidized Sb(V) is then converted to the dimethylantimony(V) porphyrin by excess $(CH_3)_3Al$.
(11) Scheer, H.; Katz, J. J. In *Porphyrins and Metalloporphyrins;* Smith, K. M., Ed.; Elsevier: Amsterdam, 1975; p 399.
(12) The mechanism of fluorination is unclear, but the rate of fluorination was very slow if a coordinating solvent such as *t*-BuOH (which does not react with $[(TPP)Sb(CH_3)(Br)]^+PF_6^-$ directly) was not added to solution. This suggests that fluorine atom transfer from PF_6^- to the central Sb ion is facilitated by an interaction of *t*-BuOH with the phosphorus atom of PF_6^- during the reaction.
(13) Guilard, R.; Lecomte, C.; Kadish, K. M. *Struct. Bonding (Berlin)* **1987**, *64*, 205.

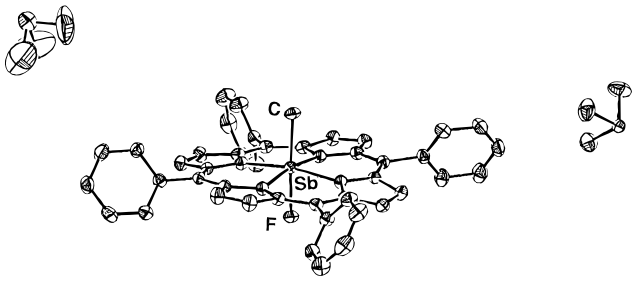

Figure 1. ORTEP diagram (30% probability ellipsoids) for $[(TPP)Sb(CH_3)(F)]^+PF_6^-$.

Table 2. Selected Bond Lengths and Angles for $[(TPP)Sb(CH_3)(F)]^+PF_6^-$

	Bond Lengths (Å)		
Sb−C(axial)	2.115(6)	Sb−F(axial)	1.928(3)
Sb−N(1)	2.088(4)	Sb−N(2)	2.086(4)
Sb−N(3)	2.085(4)	Sb−N(4)	2.086(4)
	Bond Angles (deg)		
C(axial)−Sb−F	177.7(2)	F−Sb−N(1)	84.1(2)
C(axial)−Sb−N(1)	95.6(2)	F−Sb−N(2)	84.2(2)
C(axial)−Sb−N(2)	93.5(2)	F−Sb−N(3)	85.0(2)
C(axial)−Sb−N(3)	95.4(2)	F−Sb−N(4)	84.6(2)
C(axial)−Sb−N(4)	97.7(2)	N(1)−Sb−N(2)	89.6(2)
N(2)−Sb−N(3)	89.4(2)	N(3)−Sb−N(4)	89.1(2)
N(1)−Sb−N(3)	169.0(2)	N(1)−Sb−N(4)	89.8(2)
N(2)−Sb−N(4)	168.8(2)		

different from that in $(TPP)Mo(C_6H_5)Cl$, which has been reported to lie toward the chlorine atom by 0.089 Å.[14]

An X-ray crystallographic analysis was also carried out for $[(TPP)Sb(CH_3)(OH)]^+PF_6^-$. The structure of the porphyrin ring in this compound was clearly determined, but the Sb−CH_3 and Sb−OH bond lengths could not be ascertained due to the alternate inverse arrangement of the molecules in the crystal.

Electrochemistry. The electrochemistry of each porphyrin was studied in dichloromethane or benzonitrile containing 0.1 M TBAP as supporting electrolyte. Each Sb(V) complex is stable on the cyclic voltammetry time scale, and no loss of the σ-bonded axial ligand was detected.

Typical cyclic voltammograms are shown in Figure 2, and the overall electrochemical data are summarized in Table 3. $E_{1/2}$ for the first reduction in CH_2Cl_2 ranges from −0.58 to −0.42 V for the TPP derivatives while the OEP complexes are reduced between $E_{1/2} = -0.78$ and −0.65 V. The second reduction in CH_2Cl_2 ranges from −1.05 to −0.86 V (TPP macrocycles) or from −1.28 to −1.13 V (OEP macrocycles).

The absolute potential difference between $E_{1/2}$ for reduction of the TPP and OEP complexes varies between 200 and 270 mV depending upon the specific set of axial ligands and the solvent, with easier reductions being observed for the TPP derivatives. This is in agreement with data for most OEP and TPP complexes having a variety of other central metal ions.[15] In addition, the absolute potential difference between the two reductions of a given Sb(V) complex ranges from 0.44 to 0.52 V depending upon the solvent, the macrocycle, and the specific set of axial ligands (see Table 3). This separation is similar to $\Delta E_{1/2}$ values reported for $[(TpTP)P(OCH_3)_2]^+$ and $[(TpTP)Sb(OCH_3)_2]^+$, two porphyrins which undergo electroreductions at the conjugated π ring system of the macrocycle.[16,17]

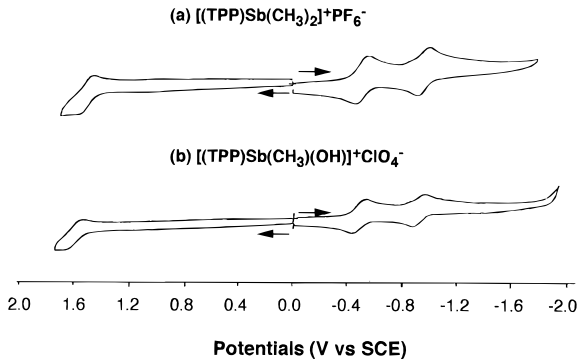

Figure 2. Cyclic voltammograms of (a) $[(TPP)Sb(CH_3)_2]^+PF_6^-$ and (b) $[(TPP)Sb(CH_3)(OH)]^+ClO_4^-$ in PhCN containing 0.1 M TBAP.

Table 3. Redox Potentials (V vs SCE) of Sb(V) Porphyrins in PhCN and CH_2Cl_2 Containing 0.1 M TBAP

solvent	macro-cycle	axial ligands		oxidn	redn		
				$E_{1/2}$	$E_{1/2}(1)$	$E_{1/2}(2)$	$\Delta E_{1/2}$(red)[a]
PhCN	TPP	CH_3	CH_3	1.51	−0.50	−0.96	0.46
			OH^-	1.60	−0.47	−0.91	0.44
			OCH_3^-	1.68	−0.43	−0.90	0.47
			F^-	1.75	−0.38	−0.83	0.45
		OCH_3^-	OH^-	1.81	−0.39	−0.84	0.45
	OEP	CH_3	CH_3	1.66[b]	−0.86	−1.38	0.52
		C_2H_5	OH^-	1.58[b]	−0.71	−1.17	0.46
		OCH_3^-	OH^-	1.28[b]	−0.66	−1.16	0.50
CH_2Cl_2	TPP	CH_3	CH_3		−0.58	−1.05	0.47
			OH^-		−0.49	−0.96	0.47
			OCH_3^-		−0.49	−0.99	0.50
			F^-		−0.43	−0.91	0.48
		OCH_3^-	OH^-		−0.42	−0.86	0.44
	OEP	CH_3	CH_3		−0.78	−1.28	0.48
		C_2H_5	OH^-		−0.74	−1.24	0.50
		OCH_3^-	OH^-		−0.65	−1.13	0.48

[a] $\Delta E_{1/2}(red) = E_{1/2}(1) - E_{1/2}(2)$. [b] Irreversible reaction; value given is E_{pa}, at 100 mV/s.

Reversible oxidations are seen for each TPP complex in PhCN (see Table 3 and Figure 2), but only irreversible processes are obtained for the three investigated OEP derivatives in this solvent. Oxidations were not reported in earlier electrochemical studies of antimony porphyrins,[13−15] and this process in the present series of compounds is assigned to a ring-centered electrooxidation.

Finally, it should be pointed out that the absolute potential difference between $E_{1/2}$ for the reversible first reduction and reversible first oxidation of the five TPP complexes ranges from 2.01 for the dimethyl derivative to 2.20 V for the OCH_3^-/OH^- complex in PhCN. These values are on the low side of the average 2.25 V HOMO−LUMO gap measured for a number of other tetraphenyl- or octaethylporphyrins,[15] but the overall electrochemical data still suggest that each electrode process involves the conjugated porphyrin macrocycle.

Spectroelectrochemistry. The UV−visible spectral changes obtained before and during thin-layer controlled-potential reduction of each TPP complex series were recorded in PhCN. Examples of the spectral changes are presented in Figure 3 for the first reductions of $[(TPP)Sb(CH_3)_2]^+PF_6^-$ and $[(TPP)Sb(CH_3)(OH)]^+ClO_4^-$, and a summary of the overall spectral data for each neutral and electroreduced porphyrin is given in Table 4.

The data in Table 4 show a significant red shift in the Q and B bands of the neutral dimethyl compound with respect to the four other investigated derivatives. The singly reduced compounds have a band located between 707 and 770 nm, and this

(14) Colin, J.; Chevrier, B. *Organometallics* **1985**, *4*, 1090.
(15) Kadish, K. M. *Prog. Inorg. Chem.* **1986**, *34*, 435.
(16) Sayer, P.; Gouterman, M.; Connell, C. R. *Acc. Chem. Res.* **1982**, *15*, 73.
(17) Liu, Y. H.; Bénassy, M. F.; Chojnacki, S.; D'Souza, F.; Barbour, T.; Belcher, W. J.; Brothers, P. J.; Kadish, K. M. *Inorg. Chem.* **1994**, *33*, 4480.

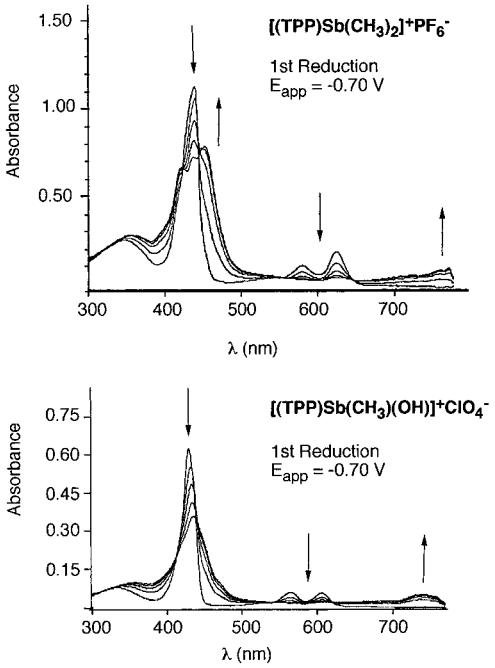

Figure 3. Spectral changes obtained upon reduction of $[(TPP)Sb(CH_3)_2]^+PF_6^-$ and $[(TPP)Sb(CH_3)(OH)]^+ClO_4^-$ in PhCN, 0.2 M TBAP. The directions of changes are shown by arrows.

Table 4. Spectral Data for Sb(V) Tetraphenylporphyrin Complexes and Their Reduction Products in PhCN Containing 0.2 M TBAP

oxidn state	axial ligands		λ, nm ($10^{-4}\epsilon$)			
neutral	CH_3	CH_3	347 (2.0)	439 (32.0)	580 (1.0)	623 (2.3)
		OH^-	336 (1.4)	429 (28.4)	565 (1.4)	606 (1.2)
		OCH_3^-	334 (1.9)	428 (39.8)	565 (1.2)	606 (1.5)
		F^-	325 (1.3)	425 (27.3)	556 (1.4)	597 (1.1)
	OCH_3^-	OH^-	319 (1.0)	425 (52.0)	554 (2.0)	594 (1.1)
singly reduced (at −0.70 V)	CH_3	CH_3	358 (2.0)	453 (22.4)[a]	770 (1.3)	
		OH^-	359 (1.7)	436 (16.2)	736 (1.0)	
		OCH_3^-	357 (2.5)	437 (35.8)	735 (1.6)	
		F^-	355 (1.8)	430 (17.7)	722 (1.1)	
	OCH_3^-	OH^-	368 (1.7)	429 (38.0)	707 (1.8)	
doubly reduced (at −1.30 V)	CH_3	CH_3	330 (2.0)[b]	453 (17.3)[c]	537 (0.9)	581 (1.0)
		OH^-	332 (1.6)	434 (10.5)	527 (0.8)	570 (0.8)
		OCH_3^-	326 (2.2)	434 (25.5)	528 (1.0)	570 (0.8)
		F^-	326 (2.0)	420 (13.9)	509 (1.5)	560 (1.4)
	OCH_3^-	OH^-	342 (1.7)	421 (23.4)	524 (1.4)	565 (1.6)

[a] Additional absorption peaks are seen at λ ($10^{-4}\epsilon$) = 439 nm (20.8) and 422 nm (19.2). [b] Additional absorption peak is seen at λ ($10^{-4}\epsilon$) = 394 nm (2.5). [c] Additional absorption peak is seen at λ ($10^{-4}\epsilon$) = 427 nm (15.4).

is consistent with an electron transfer involving the porphyrin π ring system, i.e. with formation of a porphyrin π-anion radical.[18] The changes are reversible for the first reduction of $[(TPP)Sb(CH_3)_2]^+PF_6^-$ and $[(TPP)Sb(OCH_3)(OH)]^+PF_6^-$, but this is not the case for the first reduction of $[(TPP)Sb(CH_3)(OH)]^+PF_6^-$, $[(TPP)Sb(CH_3)(OCH_3)]^+ClO_4^-$, and $[(TPP)Sb(CH_3)(F)]^+PF_6^-$, all of which show the appearance of a new band at 470 nm when the compound is reoxidized after the initial electroreduction. An example of this is seen in Figure 4. The appearance of a 470 nm band is consistent with formation of a Sb(III) complex as was reported after electroreduction of $[(TpTP)SbCl_2]^+$.[16] This oxidation state assigment is supported by the fact that all known Sb(III) porphyrins show a Soret band maximum around 460−470 nm.[16,17,19] However, the small intensity of the band suggests that the lower oxidation state

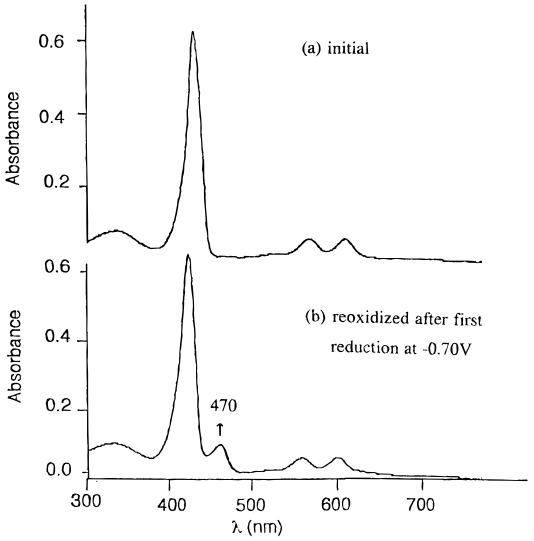

Figure 4. UV−visible spectra of (a) the initial $[(TPP)Sb(CH_3)(OH)]^+ClO_4^-$ complex and (b) the same species after reduction and reoxidation in PhCN, 0.2 M TBAP. The main difference between the two spectra is the presence of a 470 nm band in the latter case.

Scheme 4

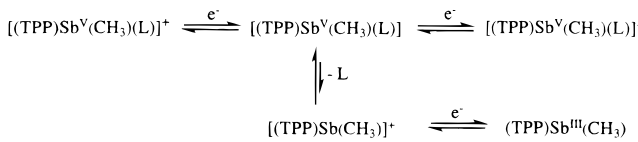

complex is present in only a minor amount. Thus, a plausible mechanism to account for the electrochemical behavior is given in Scheme 4 where L = OH^-, OCH_3^-, or F^-.

The main sequence of steps upon reduction of all five TPP complexes involves formation of the π anion radical and dianion, but a small amount (<5%) of the Sb(III) product seems to be generated after dissociation of the anionic axial ligand as shown in Scheme 4 for complexes containing one σ-bonded CH_3 group and a trans OH^-, OCH_3^-, or F^- axial ligand. The reduced $[(TPP)Sb(CH_3)_2]^+PF_6^-$ and $[(TPP)Sb(OCH_3)(OH)]^+PF_6^-$ derivatives show no evidence of a 470 nm peak, and it is therefore proposed that dissociation of the axial ligands does not occur after the initial electroreduction of these compounds.

The sequence of steps shown in Scheme 4 was confirmed by monitoring the UV−visible spectra during reduction of $[(TPP)Sb(CH_3)(OCH_3)]^+ClO_4^-$, $[(TPP)Sb(CH_3)(OH)]^+ClO_4^-$, or $[(TPP)Sb(CH_3)(F)]^+PF_6^-$ in PhCN, 0.2 M TBAP containing 1 equiv of OCH_3^-, OH^-, or F^-. These anions were added in the form of $NaOCH_3$, (TBA)OH, or (TBA)F with an aim toward supressing the ligand dissociation from electrogenerated $[(TPP)Sb^V(CH_3)(L)]$ to give $[(TPP)Sb^V(CH_3)]^+$. Under these conditions, the UV−vis spectra of the singly reduced porphyrins are identical to the spectra observed for the same compounds in PhCN not containing excess ligand. In addition, the spectral changes are reversible in the presence of excess anionic ligand in that the original Sb(V) spectrum could be seen after controlled-potential reduction and reoxidation. This also suggests that no Sb(III) porphyrin product is formed since this species would have a peak at 470 nm.

The second reduction of each TPP derivative is reversible on the thin-layer voltammetric time scale, and the spectral data of the doubly reduced porphyrins are summarized in Table 4. The shapes of the spectra are similar for all of the compounds and suggest a reduction at the conjugated π ring system of the macrocycle.

(18) Phillippi, M. A.; Goff, H. M. *J. Am. Chem. Soc.* **1982**, *104*, 6026.

(19) Knör, G.; Vogler, A. *Inorg. Chem.* **1994**, *33*, 314.

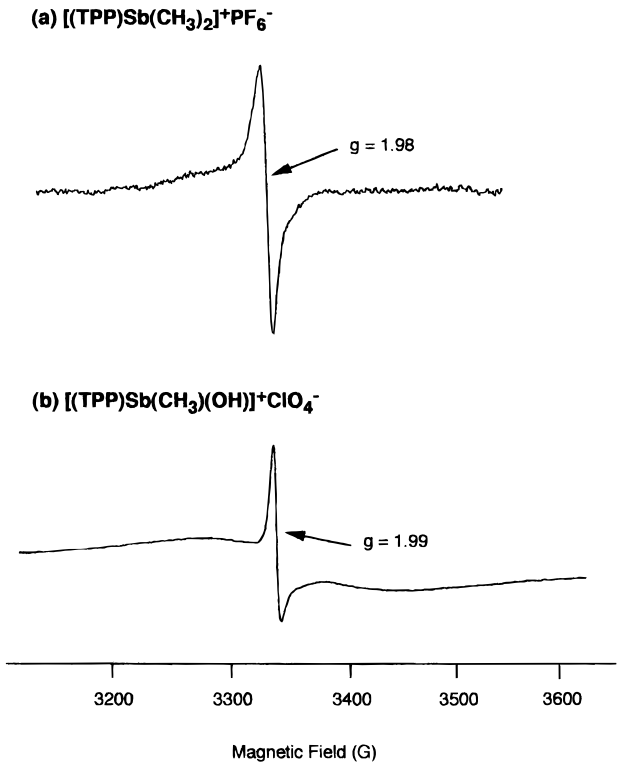

Figure 5. ESR spectra obtained at 115 K after chemical reduction of (a) $[(TPP)Sb(CH_3)_2]^+PF_6^-$ and (b) $[(TPP)Sb(CH_3)(OH)]^+ClO_4^-$ in CH_2Cl_2 using Hg/THAI[20] as a reducing agent.

ESR Characterization. An assignment of the initial electron transfer site as the porphyrin π ring system was confirmed by ESR spectra of the singly reduced tetraphenylporphyrins after chemical generation.[20] Examples of the resulting spectra are shown in Figure 5 for the case of $[(TPP)Sb(CH_3)_2]^+PF_6^-$ and $[(TPP)Sb(CH_3)(OH)]^+ClO_4^-$. Hyperfine coupling originating from an interaction of both ^{121}Sb ($I = {}^5/_2$) and ^{123}Sb ($I = {}^7/_2$) should be observed if the unpaired electrons were located on the metal,[14] but this is not observed and the isotropic signal seen in Figure 5a for $[(TPP)Sb(CH_3)_2]^+PF_6^-$ is therefore consistent with formation of a porphyrin π anion radical as the main product of the first electroreduction.

An almost isotropic ESR signal is obtained after reduction of $[(TPP)Sb(CH_3)(OH)]^+ClO_4^-$ (Figure 5b), $[(TPP)Sb(CH_3)(OCH_3)]^+ClO_4^-$, $[(TPP)Sb(OCH_3)(OH)]^+PF_6^-$, and $[(TPP)Sb(CH_3)(F)]^+PF_6^-$. There is no difference between the spectra obtained at 165 K in CH_2Cl_2 and those measured at room temperature in THF. However, the ESR signal is time-dependent in THF at room temperature. For example, the spectrum of singly reduced $[(TPP)Sb(CH_3)(OCH_3)]^+ClO_4^-$ becomes symmetrical at longer times after formation of the radical.

Finally, it should be noted that the stability of the singly reduced porphyrins is related to the type of axial ligand. The Sb(V) complexes with one or two anionic axial ligands are stable on the electrochemical time scale, but ligand dissociation occurs after the first reduction in the absence of excess anionic axial ligand. The spectroelectrochemical data suggest a small amount of Sb(III) formation, but the major reduction product is the Sb(V) porphyrin π anion radical, as evidenced by data from ESR spectroscopy.

Acknowledgment. The support of the Robert A. Welch Foundation (K.M.K., Grant E-680), The University of Houston Energy Laboratory (K.M.K.), and Grants-in-Aid for Scientific Research on the Priority Area of Organic Unusual Valency, administered by the Ministry of Education, Science and Culture of the Japanese Government (K.A., Grants 02247103, 03233104, and 04207105), is gratefully acknowledged.

Supporting Information Available: Tables of data collection and processing parameters, positional and thermal parameters, and complete interatomic distances and angles and a fully labeled ORTEP structural drawing for $[(TPP)Sb(CH_3)(F)]^+PF_6^-$ (18 pages). Ordering information is given on any current masthead page.

IC951538M

(20) Boulas, P.; Subramanian, R.; Kutner, W.; Jones, M. T.; Kadish, K. M. *J. Electrochem. Soc.* **1993**, *140*, L130.